Experimental Investigation of the Effect of Bow Profiles on Resistance of an Underwater Vehicle in Free Surface Motion

Mehran Javadi[1*], Mojtaba Dehghan Manshadi[2], Saeid Kheradmand[2] and Mohammad Moonesun[3,4]

1. Department of Mechanical Engineering, Isfahan University of Technology, Isfahan 84156, Iran
2. Department of Mechanical and Aerospace Engineering, Malek Ashtar University of Technology, Shahinshahr, Isfahan 83145/115, Iran
3. Department of Marine Science and Ocean Engineering, Malek Ashtar University of Technology, Shahinshahr, Isfahan 83145/115, Iran
4. Hydrodynamic Department, National University of Shipbuilding (NUOS), Nikolaev 35968/241, Ukraine

Abstract: In this paper, towing tank experiments are conducted to study the behavior of flow on a model of the underwater vehicle with various shapes of bows, i.e. tango and standard bows in free surface motion tests. The total resistances for different Froude numbers are considered experimentally. The towing tank is equipped with a trolley that can operate in through 0.05–6 m/s speed with ±0.02 m/s accuracy. Furthermore, the study is done on hydrodynamic coefficients i.e. total, residual and friction resistance coefficients, and the results are compared. Finally, the study on flow of wave fields around bows is done and wave filed around two bows are compared. The Froude number interval is between 0.099 and 0.349. Blockage fraction for the model is fixed to 0.005 3. The results showed that the residual resistance of the standard bow in 0.19 to 0.3 Froude number is more than the tango bow in surface motion which causes more total resistance for the submarine. Finally, details of wave generated by the bow are depicted and the effects of flow pattern on resistance drag are discussed.
Keywords: underwater vehicle; free surface motion; bow profile; residual resistance; towing tank; flow assessment; Froude number

1 Introduction

Submarines in surface motion, behave like surface ship vessels. In this condition the majority of submarine displacement volume is below the water free surface, so resistance force in surface condition motion of submarine is higher than ship. On the other hand, a submarine in surface motion experiences wave making resistance and phenomena's and flow around it are different from its submerged motion condition. Wave making resistance is caused by kinetic energy of wave. Therefore, the hydrodynamic designers of submarine vehicles strive to propose the optimum shape with the smallest amount of resistance in underwater and free surface movements. Although the submarines designed with most emphasis on their submerged performance, they have to operate on the surface for different missions. For example, battery charging and sometimes lengthy transit passages from base to its

diving area (Roy and Rydill, 1994).

Major forces acting on a submarine are skin friction drag and residual resistance. Skin friction drag is created by viscous shear drag and residual resistance drag caused due to wave making and form resistance (Bertram, 2000). For a fixed displacement volume, one idea is to reduce the wave making resistance which is the biggest part of residual resistance in free surface motion to obtain a reasonable speed.

Previous studies showed that for the deeply submerged condition, drag is associated with the viscosity of the water and form drag (Roy and Rydill, 1994). Different shapes of underwater vehicles were considered in the literature. Ellipsoid shape for submarine hull is suitable for deep submerged condition. However, this shape is inappropriate for free surface condition, where waves with high altitude are generated in the bow region. Sometimes these waves reach to sail and whole body tends to move under the surface. On the other hand, a flared and pointed bow is not a good candidate for under water operation. Experimental, analytical and numerical methods were applied to explore the optimum shape of underwater vehicles in submerged as well as surface motion. A well-known method to study of submarine surface motion resistance is the towing tank test of its scaled model.

A wide variety of shape optimizations are studied for surface and underwater vehicle. Flow measurement around a model ship with propeller and rudder for the design of hull forms show better resistance and propulsive performance (Van and Kim, 2006; Zhang, 2012). The bow wave breaking and the viscous interaction of stern wave study by simulating the free-surface flows (Kwag, 2000) and shape optimization of bow bulbs with minimum wave-making resistance based on Rankine source method (Van and Kim, 2006) are examples of shape optimization studies. The optimum shape of submarine bow and behavior of flow on a model of underwater vehicle with tango bow shape was studied by Moonesun *et al*. (2013). In this study, experimental tests in towing tank was conducted and compared with computational fluid dynamics (CFD) results and experimental formulas. The result showed the accuracy of each of six methods in the calculation of submerged

resistance of submarine and present and optimum resistance coefficient for a submarine. Optimum hull shape of an underwater vehicle moving near the surface was studied by Alvarez *et al*. (2009). Specifically, a first-order ranking panel method has been implemented to compute the wave resistance on a body of revolution moving close to the free surface. The total drag of the scaled model of the torpedo-like and resulting optimum shape was measured in towing tank. Measurements has shown a smaller resistance of the optimized shape in the range of the considered Froude number and more total drag in surface condition due to wave forced resistance. The experimental study on forces and moment on AUV hull form in the vertical plane at towing tank was done by Jagadeesh *et al*. (2009). The study was carried out at typical speeds of autonomous underwater vehicles (0.4–1.4 m/s) by varying pitch angles (0–15°). The hydrodynamic forces and moment are measured by an internally mounted multi-component strain gauge type balance. The measurements have also been used to validate results obtained from a CFD code that uses Reynolds Average Navier–Stokes equations. The study showed that the axial and normal force coefficients are increased by 18% and 195%. The drag, lift and pitching moment coefficients are increased by 90%, 182% and 297% on vehicle hull form at $\alpha = 15^{\circ}$ and $Re_{v} = 3.86 \times 10^{5}$.

Suman *et al*. (2010) designed and tested an ellipsoidal head to evaluate the functionality for improved hydrodynamic performance of an underwater vehicle. The designed vehicle having ellipsoidal heads of different major to minor axes ratio is fabricated and tested experimentally to validate the computational results. The result showed that the hydrodynamic performance of the vehicle can be improved with ellipsoidal profile head in submerged conditions. Numerical study on control effectiveness of a high-speed underwater vehicle with cruciform stern configuration using a computational fluid dynamics approach was done by Kim and Cho (2011). The calculation of the control derivatives of the underwater vehicle is validated by comparison with the experimental results of towing tank tests. The numerical results showed that the force derivatives of the vehicle are over predicted by about 5% and the moment derivatives of the vehicle are over-predicted by about 10%.

A modified Rankine source panel method was presented for solving a linearized free-surface flow problem with respect to the double body potential. The results showed that the Rankine source panel method could be an efficient tool in evaluating the flow field, wave pattern and wave resistance for various ship forms (Shahjada Tarafder *et al*. 2008). Results also showed that the calculated wave making resistance is in line with measured data. A new model for the simulation of spilling breaking waves in naval flows was presented. The model has been implemented in a finite-volume code developed for naval flows, and its performances have been validated against experimental data for a submerged profile, an S60 hull in drift motion, and the

US Combatant DTMB 5415 model on a straight course. This prevents the simulation of breaking on the shoulder and stern waves, as observed in real ship flows. In order to assess the characteristics of the model in a three-dimensional context, the wave patterns around an S60 hull in drift motion and around a DTMB 5415 model on a straight course were considered. The locations and extensions of the breakers were correctly captured in both cases. The wave damping due to breaking is also well represented. However, its effects tend to overlap with potential numerical viscosity due to the grid stretching, resulting in an excessive damping far from the hull (Muscari and Di Mascio, 2004). Xie and Ye (2011) used non linear programming to optimize the hull form of displacement type deep-vee vessels with bulbous. The total resistance was chosen as target function. The offsets of ship form are the optimizing variables. The hull form displacement and variation range of offsets are used as restrictions. The effect of sailing pose was considered to calculate the total resistance and the wave-making resistance of which was obtained by using Michell's integration. The number of chine line, which should be considered in the hull form optimization has significant influence on the resistance performance. An improved hull form which exhibited a reduction rate of 17.15% on wave making resistance, 9.52% on frictional resistance, and 12.56% on total resistance was obtained at given ship speed. It is applicable and reliable to adopt nonlinear programming for the hull optimization of displacement type deep-vee vessels.

In the current investigation, the hydrodynamic behavior of a submarine with two different bows using towing tank experiments is studied. The main objective is to find an appropriate bow shape reducing the residual resistance i.e., the minimum total resistance in free surface motion. The examination process is constrained for constant volume of the vehicle. Tango and standard bows are two types of submarines bows that have been compared in surface motion. Forces acting on the model and flow pattern specially waves near bow are reported and discussed. The formulation employed in this study is in accordance with standards presented by the ITTC method.

2 Equipments and experimental procedure

2.1 Model setup

Experiments were conducted in the towing tank which has 108 m length, 3 m width and 2.2 m depth. The basin is equipped with a trolley that's able to operate in 0.05–6 m/s speed with ±0.02 m/s accuracy. The trolley is moved by two 7.5 kW electromotor. The trolley is controlled via a wireless system from the control room of the lab. The system is prepared with proper frequency encoder, i.e., 500 pulses in minutes, which decreases the uncertainty of measurements. A three degree of freedom dynamometer is used for force measurements. The dynamometer was calibrated by calibration weights (ITTC, 2002b). Data was recorded via an

accurate data acquisition system. The dynamometer equipped with 100 N load cells that has 1% uncertainty (ITTC, 2002d). An amplifier set is used to raise signals of load cells and to reduce the noise sensitivity of the system. All data are filtered to eliminate the undesirable accelerating parts of the motion data, primary and terminative motion of the trolley. The data presented in this paper for each point is an average of several towing tank runs. For each run, at least 750 samples in 15 s were collected and ensemble averaged. Schematic of the model and the overall test set up is shown in Fig. 1.
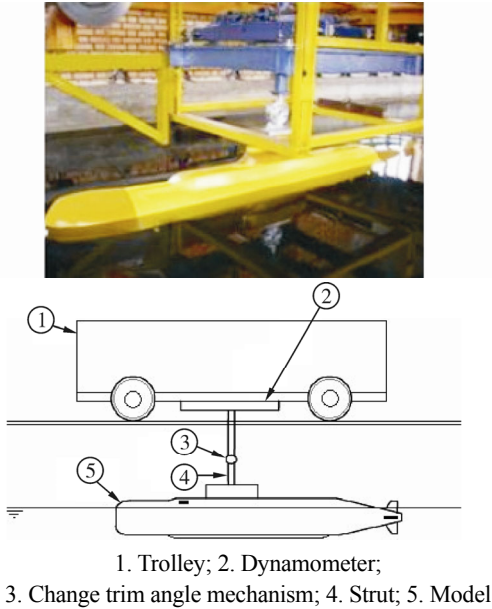

1. Trolley; 2. Dynamometer;
3. Change trim angle mechanism; 4. Strut; 5. Model

Fig. 1 Model setup in the towing

As indicated, the main purpose of the study was to explore the effect of bow shape on the hydrodynamic behavior, i.e., residual and total resistance of a submarine in surface motions. The experiment was conducted with a submarine model that was made by wood (ITTC, 2002a). For the bow effect study on total resistance, two bows with the same length are manufactured. Fig. 2 shows the profiles of the bows. Profile A and B are tango and standard bow shape, respectively. Table 1 provides a summary of the scale model characteristics.

Furthermore, the model was connected to the dynamometer with a strut rigidly to restrict yaw, pitch and other uninvited motions. The forced transition (laminar to turbulence) was achieved by installation of trip strips on the model. Trip strips (10 mm width) are installed on the bow at 5% of the overall length (Barlow *et al.*, 1999). The trim angle of the model is adjusted to equal to zero for all tests. The models dimensions are selected considering the towing tank dimensions, speed of trolley and blockage effect. Blockage fraction for the model is 0.005 3 that defined as:

$$m = \frac{a(\text{m}^2)}{A(\text{m}^2)} \qquad (1)$$

where *m* is the blockage parameter, the frontal area of the

model and *A* is the cross section area of the towing tank. The temperature in the towing tank is adjustable and it is fixed to 16 degrees of centigrade and physical condition of water measured as recommended by ITTC.
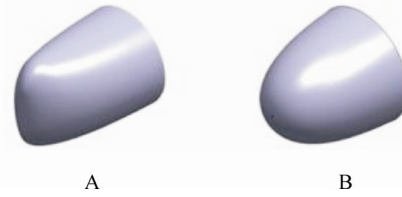

Fig. 2 The Bows profiles; tango shape (A) and standard shape (B)

Table 1 A summary of scale model characteristics

Characteristics	Quantity
Length/mm	2 110
Maximum diameter/mm	233
Length of each bows/mm	390
Draft/mm	183
Mass/kg	32

2.2 Mathematical backgrounds

Total hull resistance is split up into friction, form and wave resistance components. The friction resistance is due to viscosity. The water far from the body is at rest. There is a sharp velocity profile near the body where fluids particles are attached to the model and are traveling with model velocity (Molland *et al.*, 2011). In other words, a velocity gradient occurs in the boundary layer whilst persuades shear stresses that integrated over the wetted surface yield and lead to the friction resistance. Accurate computation of friction resistance may require an enormous computational effort. Friction resistance usually approximated by the drag generated as a result of a turbulent flow over a flat plate with the same wetted area and length of the body. The friction drag coefficient is given as (ITTC, 2002c):

$$C_F = \frac{0.075}{(\lg Re - 2)^2} \qquad (2)$$

where C_F is the non dimensional friction drag coefficient and *Re* is the Reynolds number based on the body length scale. Consequently, the friction drag is expressed as:

$$R_F = 0.5 C_F \rho S V^2 \qquad (3)$$

where *S* is the wetted surface in motionless water, *V* the model speed and ρ the density of the water of towing tank.

Using the results of the dynamometer in the towing tank, the total drag R_T can be obtained. One may write:

$$C_T = \frac{R_T}{0.5 \rho V^2 S} \qquad (4)$$

where C_T is the non dimensional total drag coefficient.

The residual drag is a significant parameter that typically

used in hydrodynamic studies. The residual drag is defined as total resistance except for skin friction drag. Residual drag coefficient is considered as:

$$C_R = C_T - C_F \tag{5}$$

where C_R is the coefficient of residual drag. Decomposition and classification of resistance in marine applications is shown in Fig. 3 which presents the different levels of resistance. A popular and well known classification in marine engineering for total resistance is the summation of wave resistance, viscous pressure resistance and friction resistance. It means $C_R = C_{vp} + C_w$.
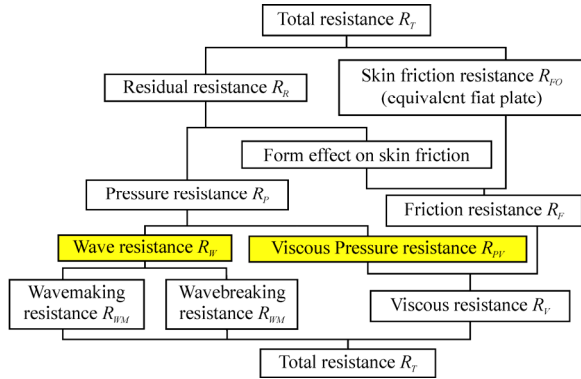
Fig. 3 Decomposition and classification of resistance in marine applications

Wave resistance drag is the biggest components (up to 50%) of residual drag in surface motions at high Froude numbers. The height of wave given as:

$$h^2 = h_f^2 + h_a^2 + 2h_f h_a \cos\varepsilon \tag{6}$$

where h, h_f and h_a are heights of average, bow and stern waves and ε is the phase difference. The wave making resistance related to the height of wave in second power. i.e. $R_W \propto h^2$ where R_W is wave making resistance. The wave length around the submarine is expressed as:

$$\lambda = \frac{2\pi V^2}{g} \tag{7}$$

where V is vehicle velocity and g is gravity. If a period of wave length extends to total length of the submarine, it is possible to consider L instead of λ. It means for an absolute period of the wave, one may write:

$$\frac{V^2}{L} = \frac{g}{2\pi} \tag{8}$$

where, for a semi period, $N\pi$ is considered instead of 2π and the equation changed to:

$$\frac{V^2}{L} = \frac{g}{N\pi} \tag{9}$$

Here, the main challenge is determination of L. In marine vehicles, there are several definitions for "length" such as:

L_{OA}, L_{WL} and L_{BP} but here some other definitions may be considered such as length between pressure centre of bow and stern (L_{CP}). Some differences in scientific sources are because of that. In Bertram (2000), L has been defined as $L = 0.9 \times L_{BP}$ (L_{BP} is the length between perpendiculars) and N is the semi period number:

$$N = \frac{0.9 L g}{V^2 \pi} \tag{10}$$

It is possible to adapt the Eq. (10) to the following equation:

$$\frac{V}{\sqrt{Lg}} = \sqrt{\frac{0.9}{N\pi}} = Fn \tag{11}$$

The variations of wave resistance coefficient versus Froude number is according to Fig.4. The reason of these non-linear variations is the situation of combination of bow wave and stern wave. As shown in Fig.4, the "Hump" positions are unsuitable conditions and "Hollow" positions are suitable conditions. Some other studies for submarines are done in Iranian hydrodynamic series of submarines (IHSS).
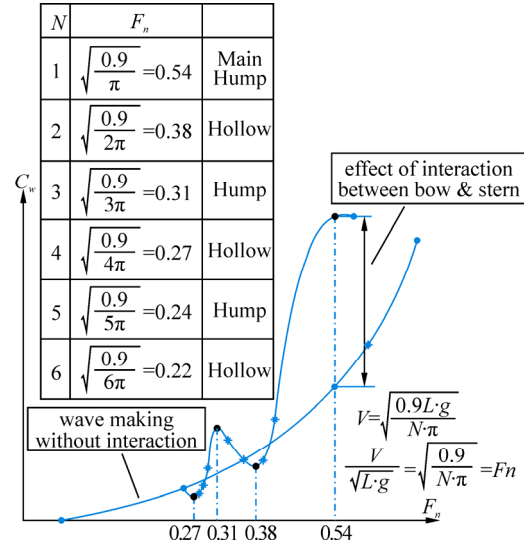
Fig. 4 Variations of wave resistance coefficient versus Froude number

An approximate formula for estimating the wave resistance is as below:

$$C_w = 3\,561.3\,Fn^6 - 8\,812.6\,Fn^5 + 8\,148.4\,Fn^4 -$$
$$3\,454.3\,Fn^3 + 654.09\,Fn^2 - 40.235\,Fn \tag{12}$$

3 Results and discussions

3.1 Force measurements

In order to investigate the effects of bow profile on hydrodynamic performance of the vehicle, total drag of the model is measured in a range of Froude numbers. Fig. 5 shows the variation of forces acting on the model versus Froude number for tango and standard bow profiles. The figure clearly shows that the total drag increases with

Froude number. Fig. 5 shows that after critical Froude number (*Fn*= 0.22), the trend of total drag decline with sharp slop, but before this Froude number, the trends of results progress such as a straight line and the variations are limited. Additionally, at low Froude number (0.098 < *Fn* < 0.22), difference between total drags caused by tango and standard bows are low (less than 1.08 N). However at higher Froude numbers (0.22 < *Fn* < 0.3), the amount of total drag for standard bow is higher than that of tango bow. Maximum difference is 3.82 N that observed at *Fn* of 0.3 where total drag of model with standard and tango bows are 16.08 N and 19.91 N respectively. At *Fn* = 0.22, total resistance increases suddenly this means that critical Froude number of this vehicle is 0.22.

The total drag is the sum of friction drag and residual resistance. Fig. 6 show the variations of these types of drag as function of Froude number in a two graph for two bows. Fig.6 show that all types of drags increase by Froude numbers. By inspection on the Figure, one can find that in *Fn* = 0.22, there is a rapid augmentation in the total resistance. In low Froude numbers, friction drag is main part of the total drag. The result shows that for the model with tango bow at *Fn* = 0.098, the residual resistance is 4 percent of total resistance. But for model with standard bow at the same Froude number, residual resistance is 33 percent of total drag. In this Froude number and for both bows, friction resistance is the biggest component of submarine total drag. By increasing Froude number to 0.197, residual resistance to total resistance ratio for tango and standard bows is 52% and 62% respectively. In Froude number between 0.3 to 0.325 residual resistances is major component of total drag for two bows.

On the other hand, the friction drag is not a strong function of Froude number for two cases. The friction drag depends on model dimensions and its wetted area. The length of the model and its wetted surface for the tango and standard bows are the same. Thus, the friction drag coefficients for two types of bows are nearly the same. Using measured data of total and calculated friction drag it is possible to find residual drag. Fig. 7 shows the variations of residual resistance coefficient against Froude number for two bows. The findings show that the quantity of the residual resistance coefficient of standard bow is more than tango shape. It is evident that there are many humps showing undesirable interactions and hallows points mentioned to the desirable interaction between bow and stern waves on the graph. One may conclude that residual resistance coefficient depends on shape of the submarine bow robustly.

Fig. 8 shows variation of total, residual and friction resistance coefficients as a function of Froude number for two bows. The graph shows that the friction coefficient for two bows is the same. Other coefficients for standard bow are bigger than the tango bow, leading to higher total resistance for submarine with standard bow. Hump and

hollow points for two bows are the same which shows that the hump and hollow points don't depend on bow shape and depend on model length. According to the graph, Frictional resistance coefficient over range of the study is limited. But the residual resistance coefficient for two bows increases by Froude number. At *Fn* = 0.22, residual resistance coefficient behaves like total resistance and has a sharp increase around this critical Froude number.
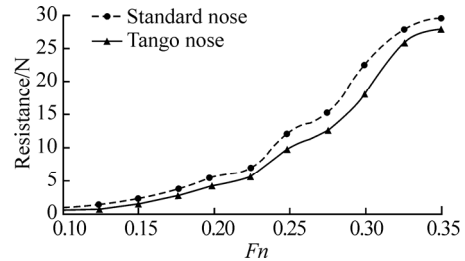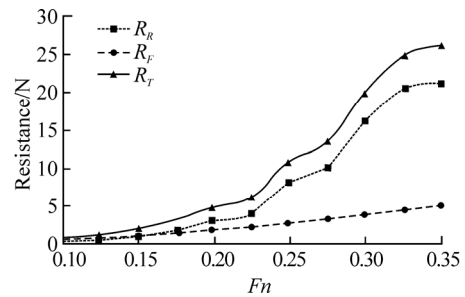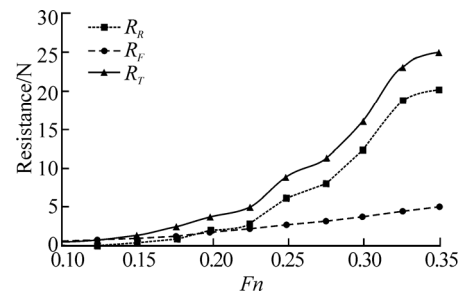

Fig. 5 Variation of total drags versus Froude number for tango and standard bows at trip conditions

(a) Standard bow

(b) Tango bow

Fig. 6 Variations of total, residual and friction drags as function of Froude number in a two graph for standard bow and tango bow
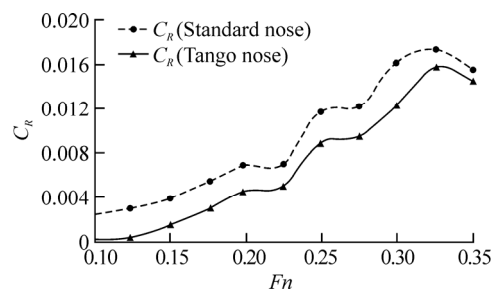

Fig. 7 Variation of residual resistance coefficient with Froude number for two cases
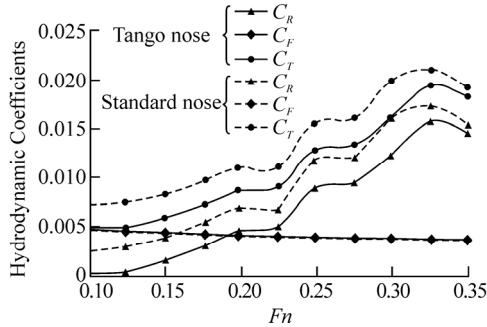
Fig. 8 Variations of hydrodynamic coefficients resistance by Froude number

3.2 Investigation of flow

Investigation of flow pattern is a significant method for fluid studies. The ability to see flow patterns around an underwater vehicle under experimental investigations often gives insight into the design and optimization process. Here, the investigation of flow experiments is performed to realize the fluid physics on and around the model with different bows. Fig. 9 shows the wave product by both bow shapes at different velocities. All patterns are obtained by a high resolution camera fixed on the trolley. Fig.10 shows the waves made by bows at the bow area of the model extended from wave crest due to high pressure stations.

The waves in aft and forward portion of shoulder are involved in low pressure stations and extended from the wave's depth. The height of waves is depended on values of velocities and increases for higher velocities. It is evident that at *Fn*= 0.099 the height of waves are very similar for both bows.

For the tango bow, with an increase in the Froude number to 0.248, the first wave crest appears at the tip of the bow where the distance between the first crest to the next crest is nearly equal to the length of the bow. At higher Froude number, the wave height from the bow and the distance between the initial crest to the next, is more than that of lower Froude numbers. Further, at *Fn*= 0.274, the waves will be collected on the top of the submarine bow. In higher Froude number (0.299 and 0.325) the water covers a part of the bow. Finally, in *Fn*= 1.59 the water covers all of bow and some part of deck.

Similar results for the standard bow for F_n= 0.099 to *Fn*= 1.59 are indicated in Fig. 9. One can find that the physics are almost the same as the tango case but the distance between the two crests is less than the tango bow and interferences of the waves are dissimilar.

In order to investigate the effect of waves on hydrodynamic performance of the vehicle consider *N*, semi period number (Eq. (9)). It is seen that for *N*=1, the bow wave started with crest and extended to wave depth of stern that can produce an undesired interference and increases the amount of wave resistance due to amplifying a low pressure region. A different phenomenon occurs for *N*=2. In this case, the waves move to the stern with the same behavior, i.e. with the crest of the wave. In other words, the crest and the

depth of the wave are neutralized or weakened in the stern due to a preferred interference. Therefore, the wave resistance may slightly change. One may conclude that the wave resistance will increase for odd values of *N* where it is almost fixed for even counterparts. The variations in the local curvatures show the interferences between the bow and stern waves in Fig. 10.
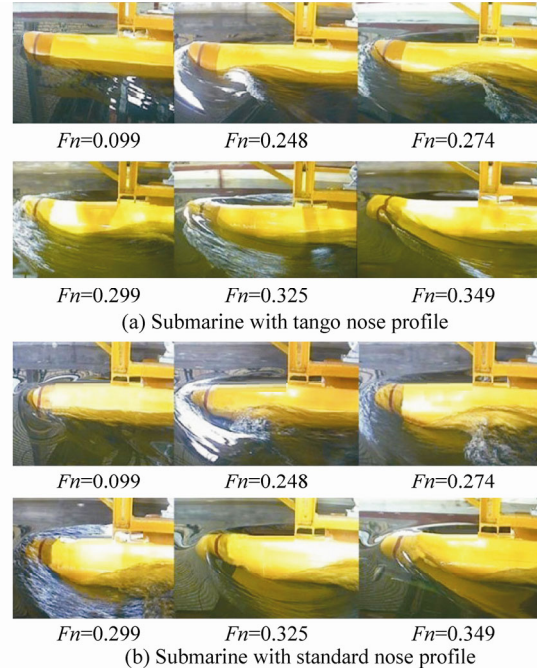

Fn=0.099   *Fn*=0.248   *Fn*=0.274

Fn=0.299   *Fn*=0.325   *Fn*=0.349
(a) Submarine with tango nose profile

Fn=0.099   *Fn*=0.248   *Fn*=0.274

Fn=0.299   *Fn*=0.325   *Fn*=0.349
(b) Submarine with standard nose profile

Fig. 9 Flow investigations of waves made by tango and standard bows in around the bow body in different Froude numbers

Fn=0.099

Fn=0.248

Fn=0.274
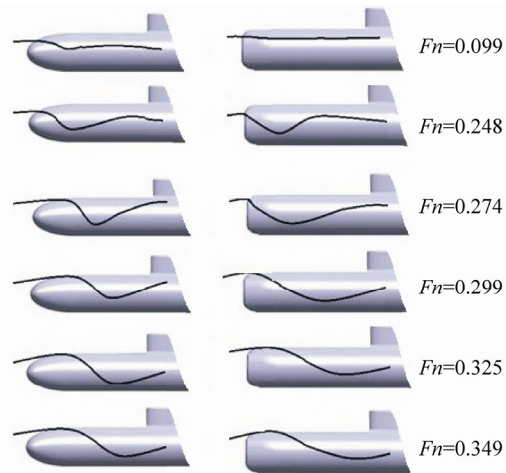
Fn=0.299

Fn=0.325

Fn=0.349

Fig. 10 The trajectories of the waves from bow to stern of the model with the both types of bows at different velocities

If one can to cancel out these interferences, the waves follow a parabolic route without any local changing. Moreover, the resistance increases with the raise of velocity. The trajectories of the waves from bow to stern of the model with both types of bows at different velocities are shown in Fig. 8.

The results showed that the tango shape bow has the main effect on the wave breakage and decreases the resistance of the model more than the other bow shape. Also, for higher velocities, the height and length of the waves will increase. The profiles of bow and the Froude number have a significant role in the resistance of the model. Looking at the results, the tango shape bow creates desirable behavior for waves and reduces the resistance relatively to standard bow at the same Froude number. One may conclude that there are two reasons for resistance reduction due to decrease in the height of the wave. Firstly, the reduction of the wave height can decrease wave making resistance. Secondary, wave height reduction can also prevent the production of wave in critical conditions and undesirable interactions.

Fig. 11 shows variations of portion of the wave making resistance to the total resistance for the model with different types of bows. The results clearly showed that for lower velocities, there is a significant difference of wave resistance between tango and standard shapes of bows. However, at higher velocities this difference is less and is related to the length and the displacement volume of the submarine. The results showed that in low and middle Froude number (Fn= 0.098–0.3), the height of wave caused by the tango bow is smaller than the standard bow. Therefore, the tango bow is more suitable for submarine in free surface motions.
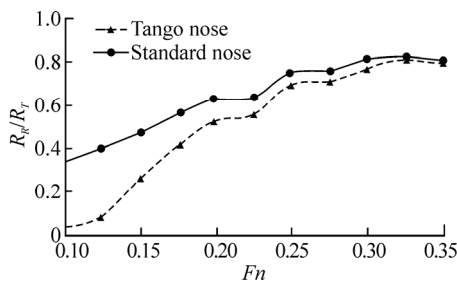

Fig. 11 Variations of the portion of the wave making resistance to the total resistance for the model

4 Conclusions

Experiments were performed to study the behavior of flow around a model of submarine with two types of bow shapes. The two types of bow shapes consisted of tango and standard bows in free surface tests. The resistance components for different Froude numbers were considered. Finally, flow visualizations of wave fields around bows are done and wave filed around two bows are compared. The Froude numbers were varied between 0.099 and 0.349. The trim angle of the model is adjusted equal to zero for all Froude numbers. Blockage fraction for the model is fixed to 0.005 3. The following conclusions are obtained in this investigation:

1) The residual resistance of the standard bow is higher than the tango bow in surface motion that caused more total resistance for the submarine. However, in high Froude, bow shape effect decreases and the total resistance depends on submarine's length and displacement.

2) The results showed that the role of residual resistance is over 80 percent of the total drag in larger Froude numbers where the variations of the friction drag with Froude number are slightly increased. Furthermore, the length of the model and wetted surface for the tango and standard bows are the same. Thus, the amount of friction drag coefficients for two types of bows is closely near.

3) The patterns of flow from visualization showed that the waves made by bows at bow and stern areas of the model extended from wave crest due to high pressure stations. While, the waves in aft and forward portion of shoulder are involved in low pressure stations and extended from waves depth. The height of waves is depended on values of velocities and increases for higher velocities. Also, for the standard bow, the distance between two crests is less than the tango bow and interferences of the waves are dissimilar.

4) The profiles of the bow and the Froude number played a significant role in the resistance of the model. Here, the tango shape bow created desirable behavior for waves and caused the least resistance relatively to standard bow at the same Froude number.

Nomenclatures

A	Cross section area of towing tank (m^2)
a	Cross section area of model (m^2)
C_F	Friction resistance coefficient
C_T	Total resistance coefficient
C_w	wave resistance coefficient
C_{vp}	Viscous resistance coefficient
C_R	Residual resistance coefficient
h	Combined wave height (m)
h_a	Stern (aft) wave height (m)
h_f	Bow (fore) wave height
L	Length in Froude number (m)
L_{OA}	Length overall (maximum length) (m)
L_{BP}	Length between perpendiculars (m)
L_{WL}	Level waterline length
L_{CP}	Length of center of pressure
N	Semi period number
R	Resistance or drag (N)
Re	Reynolds number
S	Wetted surface area (m^2)
V	Speed of model (m/s)
λ	Wave length (m)
ρ	Water density (kg/m^3)

References

Alvarez A, Bertram V, Gualdesi V (2009). Hull hydrodynamic optimization of autonomous underwater vehicles operating at snorkeling depth. *Jordan Journal of Ocean Engineering*, **36**(1), 105-112.
DOI: 10.1016/j.oceaneng.2008.08.006

Barlow JB, Rae WH, Pope A (1999). *Low-speed wind tunnel testing*. 3rd edition. John Wiley & Sons, New York, USA, 609-649.

Bertram V (2000). *Practical ship hydrodynamics*. 1st edition. Butterworth-Heinemann, Kidlington, Oxford, UK, 68-117.

ITTC (2002a). Recommended procedures and guidelines—Model manufacture ship models. *Proceedings of the 23rd International Towing Tank Conference*, Venice, Italy, 7.5-01-01-01.

ITTC (2002b). Recommended procedures and guidelines—Sample work instructions calibration of load cells. *Proceedings of the 23rd International Towing Tank Conference*, Venice, Italy, 7.6-02-09.

ITTC (2002c). Recommended procedures and guidelines—Testing and extrapolation methods resistance: Resistance test. *Proceedings of the 23rd International Towing Tank Conference*, Venice, Italy, 7.5-02-02-01.

ITTC (2002d). Recommended procedures and guidelines—Testing and extrapolation methods resistance: Uncertainty analysis, example for resistance test. *Proceedings of the 23rd International Towing Tank Conference*, Venice, Italy, 7.5-02-02.

Jagadeesh P, Murali K, Idichandy VG (2009). Experimental investigation of hydrodynamic force coefficients over AUV hull form. *Ocean Engineering*, **36**(1), 113-118.
DOI: 10.1016/j.oceaneng.2008.11.008

Kwag SH (2000). Bow wave breaking and viscous interaction of stern wave. *Journal of Mechanical Science and Technology*, **14**(4), 448-455.
DOI:10.1007/BF03186439

Kim H, Cho H (2011). Numerical study on control derivatives of a high-speed underwater vehicle. *Journal of Mechanical Science and Technology*, **25**(3), 759-765.
DOI: 10.1007/s12206-011-0123-7

Molland AF, Turnock SR, Hudson DR (2011). *Ship resistance and propulsion*. Cambridge University Press, New York, USA, 14-15.
DOI: 10.1017/CBO9780511974113

Moonesun M, Javadi M, Charmdooz P, Mikhailovich KU (2013). Evaluation of submarine model test in towing tank and comparison with CFD and experimental formula for fully submerged resistance. *Indian Journal of Geo-Marine Sciences*, **42**(8), 1049-1056.

Muscari R, Di Mascio A (2004). Numerical modeling of breaking waves generated by a ship's hull. *Journal of Marine Science and Technology*, **9**(4), 158-170.
DOI: 10.1007/s00773-004-0182-x

Roy B, Rydill L (1994). *Concepts in submarine design*. Cambridge University Press, London, UK, 104-124.

Shahjada Tarafder M, Suzuki K (2008). Numerical calculation of free-surface potential flow around a ship using the modified Rankine source panel method. *Ocean Engineering*, **35**(5-6), 536-544.
DOI: 10.1016/j.oceaneng.2007.11.004

Suman KNS, Nageswara D, Das HN, Bhanu Kiran G (2010). Hydrodynamic performance evaluation of an ellipsoidal bow for a high speed under water vehicle. *Jordan Journal of Mechanical and Industrial Engineering*, **4**(5), 641-652.

Van SH, Kim WJ (2006). Flow measurement around a model ship with propeller and rudder. *Journal of Experiments in Fluids*, **40**(4), 533-545.
DOI: 10.1007/s00348-005-0093-6

Xie Yi, Ye Qing (2011). Hull form optimization of displacement type deep-vee vessels based on nonlinear programming. *International Conference on Electrical and Control Engineering (ICECE)*, Yichang, China, 2266-2269.
DOI: 10.1109/ICECENG.2011.6057745

Zhang Baoji (2012). Shape optimization of bow bulbs with minimum wave-making resistance based on Rankine source method. *Journal of Shanghai Jiaotong University*, **17**(1), 65-69.
DOI: 10.1007/s12204-012-1239-3